Cement and Concrete Research 124 (2019) 105857

Contents lists available at ScienceDirect

Cement and Concrete Research

journal homepage: www.elsevier.com/locate/cemconres

Structural build-up of cementitious paste with nano-Fe_3O_4 under time-varying magnetic fields

Dengwu Jiao[a,b], Khadija El Cheikh[a], Caijun Shi[b], Karel Lesage[a], Geert De Schutter[a,*]

[a] Magnel Laboratory for Concrete Research, Department of Structural Engineering, Ghent University, 9052 Ghent, Belgium
[b] Key Laboratory for Green and Advanced Civil Engineering Materials and Application Technology of Hunan Province, College of Civil Engineering, Hunan University, Changsha 410082, China

ARTICLE INFO

Keywords:
Cement paste
Structural build-up
Magnetic field
Small amplitude oscillatory shear
Nano-Fe_3O_4

ABSTRACT

The structural build-up of cementitious paste with nano-Fe_3O_4 under time-varying magnetic fields was experimentally investigated using small amplitude oscillatory shear (SAOS) technique. Several modes of magnetic fields, such as constant, sudden-changed and linearly-changed, were applied to the cementitious paste. Results showed that the structural build-up of the cementitious paste depended on the magnetizing time and magnetic field strength. Applying constant magnetic fields improved the liquid-like behavior during first minutes and afterwards the solid-like property was enhanced. Both the sudden-increased and sudden-decreased magnetic fields resulted in a sharp decrease in storage modulus. The linearly increasing magnetic field resulted in a slight increase in storage modulus but higher liquid-like behavior. When the magnetic field was linearly decreased from 0.5 T to approx. 0.25 T, the structural build-up was enhanced significantly, and with the continuously decreasing magnetic field from approx. 0.25 T to 0 T, a decrease in storage modulus was observed.

1. Introduction

The cement production of the European Union in 2016 increased to 169.1 million tons, ranking third behind China and India, according to the activity report (2017) published by the European Cement Association (CEMBUREAU). It can be easily forecast that cement and concrete will remain among the most commonly-used civil engineering materials in infrastructure construction in the next few decades. In order to reduce the production cost of cement and concrete, preference is given to local raw materials, which to a certain extent limits the selection of excellent materials. Consequently, a large number of mixture design methods are proposed to optimize concrete properties to meet requirements for construction [1,2]. Furthermore, construction processes play an important role in the quality control of concrete. As is well known, the engineering application processes of concrete include transporting, pumping and formwork casting. Each process is a significant factor influencing the properties of fresh and hardened concrete. However, for the same concrete mixture proportion, once the concrete is prepared, its properties become hard to be controlled to a certain extent. In this case, this concrete will be transported and pumped according to its original properties, and the construction techniques will become the main barrier to improve the robustness of concrete. More attention should be paid to improvement of construction techniques.

With the widespread use of mineral additions and chemical admixtures, self-compacting concrete (SCC) with low energy consumption and obsolete vibration is developing rapidly. However, the practical engineering applications of SCC are still unsatisfying, due to the limitation of traditional production processes. Take the pumping operation as an example, it has become an indispensable part of construction process of concrete, especially for SCC and high-performance concrete (HPC). Although many researchers have focused on the characterization of flow regime inside the pipe and the prediction of pumping pressure [3–5], there are still some challenges in the pumping operations, such as the sensitivity of human factors, impacts of bends and reducers, aggregate segregation and blocking, and the changes of rheological properties [6,7]. Furthermore, many conflicts and contradictions in requirements of fresh concrete performances exist in different operation processes. For example, lower thixotropic structural build-up is needed to overcome the major problem in resuming pumping operations if a short interruption is experienced (such as the delay of concrete truck) [8] and improve the interface properties during multi-casting process [9]. By contrast, higher structuration rate of fresh concrete is beneficial for reducing formwork pressure at the casting process [10,11]. Thus, advanced casting techniques should be proposed to satisfy future challenges. In this context, an innovative casting

* Corresponding author.
E-mail address: Geert.DeSchutter@UGent.be (G. De Schutter).

https://doi.org/10.1016/j.cemconres.2019.105857
Received 26 October 2018; Received in revised form 31 July 2019; Accepted 6 August 2019

concept "SmartCast" has been proposed by De Schutter [12,13] to overcome aforementioned problems. By actively controlling the rheology and stiffness, the structuration rate of fresh concrete could be adjusted artificially according to the requirements at different operation processes for the same concrete mixture, which could make the pumping and casting processes smarter and more reliable.

Magnetorheological (MR) fluids, first introduced by Rebinow [14], are kinds of smart materials, whose rheological behavior could be controlled by applying external magnetic fields. MR fluids are complex suspensions composed of magnetic particles and carrier fluid (Newtonian fluid). In the presence of magnetic field, the magnetic particles align along the direction of the magnetic field and chain-like or columnar structures are formed, resulting in higher elastic behavior of the suspension [15,16]. After removing the external magnetic fields, the chain-like structure breaks down and the MR fluids reversibly change from semi-solid state to liquid state. Based on the excellent characteristics (rapid, reversible and magnetic-controllable, etc.), MR fluids have been successfully applied in devices such as dampers, valves and brakes [16]. However, due to a big difference in density between magneto particles and carrier fluid, the sedimentation is the greatest challenge for widespread use of conventional MF fluids in industrial applications. Many stabilization methods, such as coating particles, adding chemical additives and using yield-stress fluid as carrier, have been proposed to improve the stability of MR fluids. Fresh cementitious paste is usually regarded as a concentrated suspension with yield stress [17–19]. A stable MR fluid could be obtained when using fresh cementitious paste as the carrier fluid. Conversely, the rheology and stiffness of cementitious paste containing magnetic particles would become controllable.

Portland cement is a kind of cementitious material composed of C_3S, C_2S, C_3A and C_4AF. In the phases of C_3A and C_4AF, there exist rich impurity iron and Fe_2O_3. The Fe_2O_3 compound has a strong tendency to dissociate into Fe^{2+} and Fe^{3+} [20]. After water is in contact with cement particles, the C_3A and C_4AF start to hydrate with gypsum to form ettringite. During these hydration processes, the dissolution concentrations of iron increase, resulting in cement paste exhibiting a slight magnetic behavior [21]. Nair and Ferron [22] pointed out that the saturation magnetization value of Portland cement with Fe_2O_3 content of 2.7% is 0.7 emu/cm^{-3}, which is far less than that of carbonyl iron powder (1700 emu/cm^{-3}). As a result, under extremely low shear strain, the rheological properties such as storage modulus and static yield stress of pure Portland cement paste only showed a limited change under external magnetic fields. Thus, magnetic particles should be added into the cement paste in view of controlling the rheological behavior of cementitious paste by applying external magnetic fields. Nair and Ferron [22,23] investigated the magnetorheological behavior of cement-based materials containing carbonyl iron powder from a long-term view. It is found that the magnetorheological behavior of cementitious paste was correlated to the external magnetic fields and the concentrations of carbonyl iron powder. The rheological properties of cementitious paste did exhibit field sensitivity with the magnetic field which was step-wise varied. However, the early structural evolution of cementitious paste is still unclear right after applying external magnetic fields. In order to achieve the goal of actively triggering the rheology and stiffness of fresh concrete, it is necessary to comprehensively understand the magnetorheological behavior of cementitious paste under the application of magnetic fields.

Ferroferric oxide (Fe_3O_4) is a ferromagnetic material with Fe^{2+} and Fe^{3+}, and the addition of nano-Fe_3O_4 accelerates the chemical hydration [24], increases the compressive strength [25,26] and reduces the water adsorption as well as the chloride penetration [27]. The magneto dipoles in the ferroferric oxide could be aligned along the external magnetic fields. Thus, it is reasonable and feasible to regulate and control the rheological behavior of cementitious paste by applying external magnetic fields. In the present study, the structural build-up of cementitious paste containing nano-Fe_3O_4 was experimentally investigated under time-varying magnetic fields. The time-sweep test with low shear strain within the linear viscoelastic region was conducted to characterize the structural build-up of cementitious paste. Several modes of magnetic fields, such as constant, sudden-changed and linearly-changed, were separately applied to the cementitious paste. This study provides some preliminary concepts that will contribute to actively controlling the rheology and stiffness of fresh concrete.

Table 1
Chemical composition of Portland cement.

Components	% by mass
SiO_2	19.6
Al_2O_3	4.88
Fe_2O_3	3.14
CaO	63.2
MgO	1.8
SO_3	2.9

2. Experimental program

2.1. Raw materials and mixture proportions

CEM I 42.5 Portland cement (OPC) conforming to EN 196-1 [28] was used in this study. The Blaine fineness is 279.5 m^2/kg and the chemical composition is shown in Table 1. Spherical Iron Oxide Fe_3O_4 Nanoparticles with Fe_3O_4 purity higher than 98% (from US Research Nanomaterials, Inc) were used as nano fillers. The average particle size and density of nano-Fe_3O_4 are 20–30 nm and 4.95 g/cm^3, respectively. All samples were prepared using de-ionized water. The water-to-cement (w/c) mass ratio of cement paste medium was 0.4. The content of nano-Fe_3O_4 was fixed at 5% by the mass of cement paste.

2.2. Mixing procedure

The cementitious pastes were mixed using a rotational rheometer with a helix geometry. The geometric parameters of the helix rotator are shown in Fig. 1. The advantage of this mixer is the low volume of applicable material, which is not the case for the commonly-used blender. The mixing procedure was set as follows: The mixed cement and nano-Fe_3O_4 were first added into the container with diameter of 28 mm and height of 70 mm. Afterwards, all of the water was poured into the container and then the helix geometry was gradually lowered into the sample at descending and rotational speed of 1 mm/s and 1000 min^{-1}, respectively. After that, the shear rate was gradually increased from 0 to 3000 min^{-1} within 30 s, and then kept mixing for 120 s at rotational speed of 3000 min^{-1}. About 15 ml of paste was prepared for each batch. The measured shear stress of cementitious pastes (w/c = 0.4, 5% nano-Fe_3O_4) during mixing is depicted in Fig. 2. It can be observed that the mixing procedure used in this study provided repeatable initial state of paste samples for the same mixture proportion.

2.3. Testing methods

The structural evolution of cementitious paste was characterized by storage modulus and phase angle, obtained from small amplitude oscillatory shear (SAOS) test using a rotational parallel plate rheometer (MCR 102, Anton Paar, Austria). The disc diameter is 20 mm and the gap between the upper and lower plates is fixed at 1 mm. During the rheological tests, the temperature was controlled at 20 ± 0.5 °C. To determine the linear viscoelastic region, strain-sweep test with strain amplitude from 0.0001% to 10% and constant frequency of 2 Hz was first conducted in the absence of magnetic fields, as shown in Fig. 3. It can be observed that the critical strain amplitude of cementitious pastes was about 0.004%, which was consistent with the order of 10^{-5} obtained in [29,30]. Thus, the strain amplitude of 0.001% was selected in

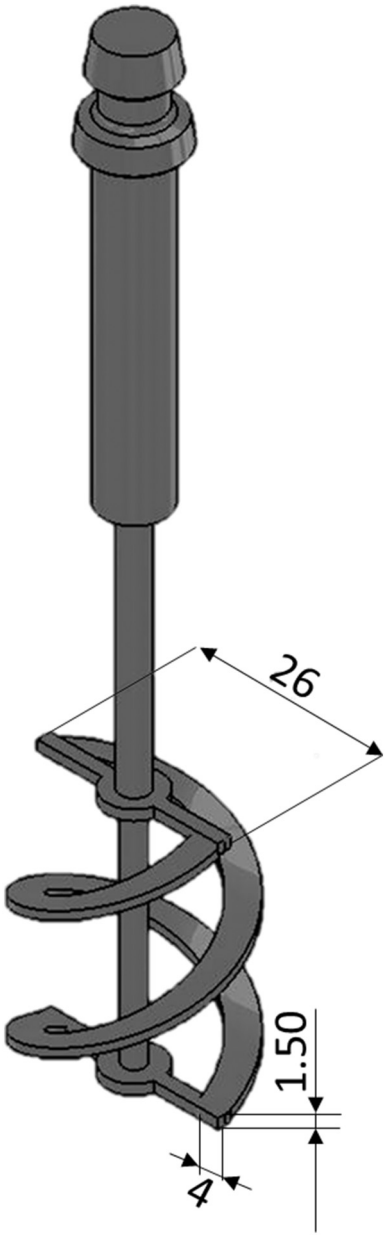

Fig. 1. The geometric parameters of the helix geometry in mm.

the time-sweep measurement.

After the sample was prepared, it was poured into the rheometer. To obtain a repeatable state and eliminate the possible influences during gap positioning, the sample was first pre-sheared at rotational speed of 100 s^{-1} for 30 s. Afterwards, the time-sweep test was immediately carried out for 15 min under given magnetic fields. Further details about the magnetic field modes will be stated in next sections. The data is recorded every second. After the test, the cementitious pastes between the plates were examined, and no obvious bleeding and agglomeration were observed. To ensure the repeatability, three rheological reproducible tests on three alternative samples were conducted.

3. Results and discussion

3.1. Constant magnetic fields

Figs. 4(a–b) show evolutions of storage modulus and phase angle of cementitious paste under constant magnetic fields. The experimental results of pure Portland cement paste with w/c of 0.4 under external

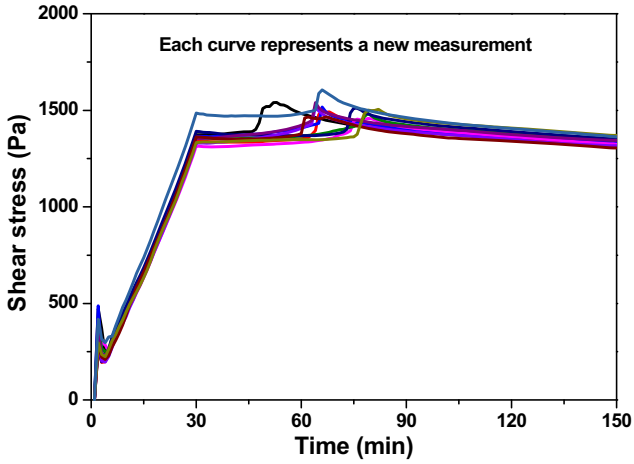

Fig. 2. Measured shear stress of cementitious pastes (w/c = 0.4, 5% nano-Fe_3O_4) during mixing procedure.

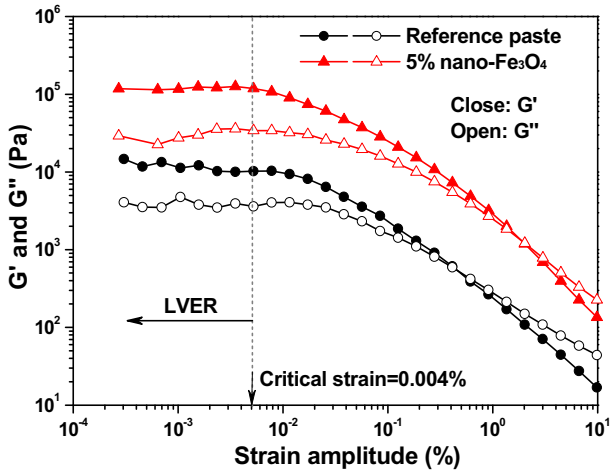

Fig. 3. Determination of linear viscoelastic region (LVER).

magnetic field of 0 T was also presented as a reference (Ref). The storage modulus of the reference cement paste gradually increased and the phase angle gradually decreased with resting time. The results are in agreement with those shown in Refs. [31–33]. Indeed, in the paste suspension, there exist Brownian forces, inter-particle interaction forces (such as electrostatic or steric repulsion and van der Waals forces), hydrodynamic force, gravitational and inertial forces. Compared to the strong inter-particle interaction forces, the Brownian motion and inertial forces can be neglected [30,34]. At rest, on one side, colloidal interactions due to the van der Waals attractive forces lead to formation of flocculated structures. On the other side, C-S-H links and bridges between cement particles are enhanced with progress of cement hydration. As a result, the rigidity and stiffness of cement paste suspensions are consolidated, exhibiting a gradual increase in storage modulus and reduction in phase angle. With the elapses of resting time, the storage modulus reached a steady increase and the phase angle also gradually stabilized, reflecting the transition from viscous behavior to elastic behavior. The time when the phase angle starts to stabilize or the storage modulus starts to increase steadily is defined as percolation time, which can be used to describe the time for colloidal particles to reach their equilibrium positions [29]. The percolation time can be quantitatively obtained from decreasing rate of phase angle. Take cementitious paste without magnetic field as an example, the decreasing rate of phase angle were around 1.12°/s and 0.03°/s in magnetization time of 5–30 s and 30–100 s, respectively. Therefore, the percolation time can be regarded as approx. 30 s. It should be noted that the

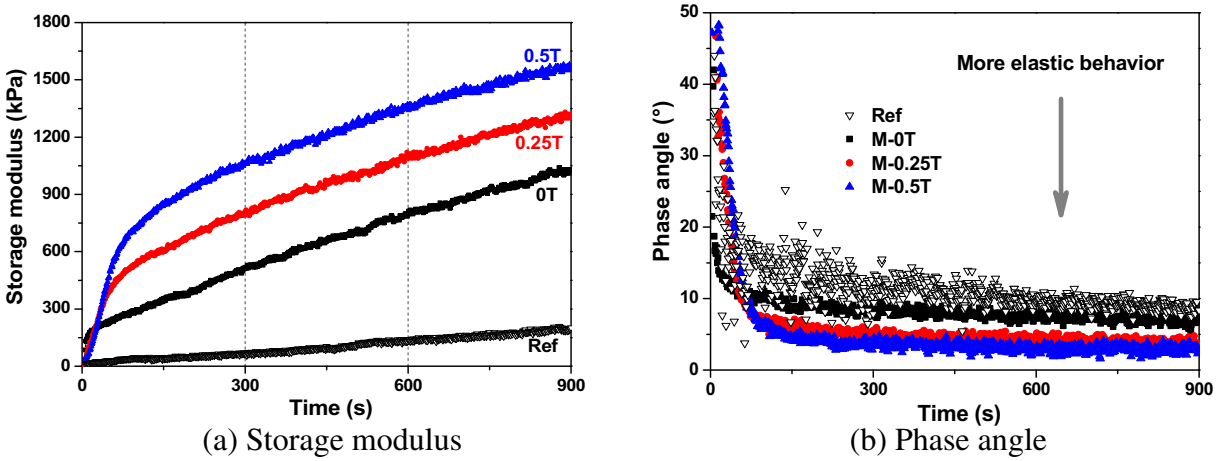

(a) Storage modulus (b) Phase angle

Fig. 4. Structural evolution of cementitious paste under constant magnetic fields.

percolation time of reference cement paste was difficult to be determined from the storage modulus and the phase angle, which can be attributed to higher liquid-like property compared to cementitious paste containing nanoparticles.

The addition of 5% nano-Fe_3O_4 significantly increased the storage modulus and resulted in more elastic behavior. This result is consistent with the conclusion reached by Nair and Ferron [22], which showed that the incorporation of 4% carbonyl iron powder significantly increased the storage modulus of cementitious paste. This can be explained by the increase of volume content of solid particles. After adding nanoparticles into cement paste medium, the average distance between particles dramatically decreases and therefore the magnitude of van der Waal forces increases. Consequently, the strength of flocculated structure is improved. As well, the addition of nanoparticles results in higher inter-particle contacts and increases the friction between particles due to the micro-filling effect. Furthermore, the reduction in free water and the strong tendency to agglomerate are also responsible for the increase in rigidity, because of the high specific surface area and high magnetic properties of nano-Fe_3O_4 [35]. The application of external constant magnetic fields increased the percolation time (for instance, ~30 s and ~150 s for magnetic fields of 0 T and 0.5 T, respectively) and storage modulus at steady state. As well, after magnetization for about 200 s, the growth rate (slope) of storage modulus is similar for different strengths of constant magnetic fields. This is explained by the fact that the rigidity of cementitious paste with 5% nano-Fe_3O_4 under the action of constant magnetic fields was related to the magnetic field strength. It is worth mentioning that the magnetizing effect of water was not considered in this study. Su and Wu [36,37] found that the flowability of fresh mortar with magnetizing water treated under 0.6 T was only increased from 180 mm to 189 mm. Thus, the possible breakdown of hydrogen bonding and water clusters in the cementitious paste was negligible compared to the magnetodynamic forces between magnetic particles.

It can be seen that higher magnetic field strength resulted in higher storage modulus and lower phase angle, i.e. higher elastic behavior. On one hand, the amount of magnetic nanoparticles that formed chains increased with the magnetic field strength. On the other hand, the bonding between magnetic nanoparticles increased with the magnetodynamic forces. Thus, higher solid-like behavior was observed at higher magnetic field strength. Once the chain-like structure formed, the storage modulus increases due to the colloidal interactions between particles. However, the storage modulus and phase angle at the beginning after applied constant magnetic fields exhibited an opposite behavior, as shown in Figs. 4(a–b). More specifically, the structural build-up rates at the beginning of applied magnetic fields, if defined by the growth rate of storage modulus from 5 s to 10 s, were 24.8, 15.2 and 6.8 kPa/s for the magnetic field strength of 0 T, 0.25 T and 0.5 T, respectively. This means that the applications of constant magnetic fields resulted in more liquid-like property at early age. This behavior paradox will be explained in the coming sections.

3.2. Sudden-changed magnetic fields

To understand the effects of external magnetic fields on the structural evolution thoroughly and systematically, three modes of sudden-changed magnetic fields were separately applied to the fresh cementitious paste. The application modes of magnetic fields are presented in Table 2.

3.2.1. Sudden-increased magnetic fields

Fig. 5 presents the evolution of storage modulus of cementitious paste (w/c = 0.4 and 5% nano-Fe_3O_4) under sudden-increased magnetic fields (modes I and II). When the magnetic field strength raised from zero to higher value (0.25 T or 0.5 T), the storage modulus experienced an abrupt decrease to a value close to that of reference cement paste (without nanoparticles and without magnetic field). This means that the structure of cementitious paste was disrupted. Afterwards, a marked increase in storage modulus was observed, indicating higher structural build-up with resting time. A similar phenomenon was also observed by Nair and Ferron [23] but no further explanation was given. This behavior obtained in our results can be explained by the distributions of nano-Fe_3O_4 particles in the cement paste matrix. In the absence of magnetic fields, the nano-Fe_3O_4 particles were randomly distributed, as illustrated in Fig. 6(a). After application of external magnetic fields, the magnetic dipoles in the nano-Fe_3O_4 will move to be aligned along the direction of magnetic field in a short time, as shown in Fig. 6(b). During their displacement to form a chain-like structure, the nanoparticles create a sort of mechanical agitation, and then the C-S-H bridges and flocculated networks between cement particles are destroyed. Furthermore, the entrained water in the agglomerated nanoparticle clusters is released, which increases the water film thickness and free water content. Thus, the cement particles transform from flocculated state to a more dispersed state. This explains the sharp

Table 2
Application modes of sudden-changed magnetic fields.

Modes	Magnetic field strength (T)		
	0–300 s	300–600 s	600–900 s
I	0	0.25	0.5
II	0	0.5	0.5
III	0.5	0.25	0

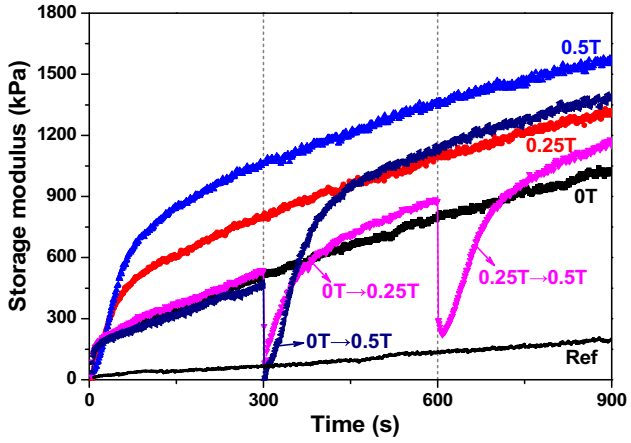

Fig. 5. Structural evolution of cementitious paste under sudden-increased magnetic fields.

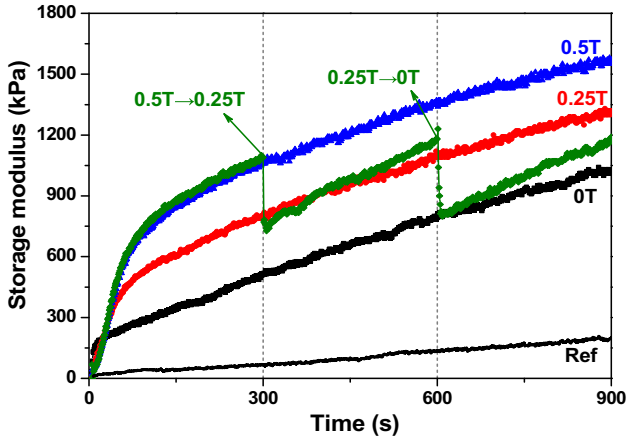

Fig. 7. Structural evolution of cementitious paste under sudden-decreased magnetic fields.

decline in storage modulus. After the chain-like structure is formed, the particles will interact again at rest and the storage modulus exhibits an increase. With the increase of magnetic field strength, the chain-like structure evolved into stronger columns-like structure, which should be responsible for the increase in storage modulus at high magnetic field strength.

The sharp decrease in storage modulus in mode I - at 600 s - when increasing the magnetic fields from 0.25 T to 0.5 T is explained by the fact that when the strength of magnetic field increases, the nanoparticles which were already in the chain-like structure will agitate and redistribute to form stronger chains or clusters. This movement will break down the links between clogged particles and lead to a decrease in storage modulus. Another explanation could be that the magnetic field of 0.25 T is not strong enough to insert all the nanoparticles in the chain-like structure. Thus, some particles will remain in the cement paste matrix. When the magnetic fields increase to 0.5 T, the remaining nanoparticles will contribute to the formation of the chains or clusters. Their movement leads to a decrease in the storage modulus of cementitious paste. From Fig. 5, it can also be seen that the abrupt decrease in storage modulus at 600 s (0.25 T to 0.5 T) was larger than that at 300 s (from 0 T to 0.25 T), indicating a higher breakdown of C-S-H networks when changing the magnetic field to a higher value. However, a higher storage modulus was still observed at 600 s. This behavior is possibly due to connections between particles in the cement paste medium strengthened with the elapsed time.

3.2.2. Sudden-decreased magnetic fields

Fig. 7 shows structural evolution of cementitious paste under the external magnetic fields with mode III (sudden-decreased magnetic fields). It can be seen that the storage modulus exhibited a drop decrease when the magnetic fields changed from high to low strength value. This expected decrease indicated that the sudden decreasing magnetic fields resulted in higher liquid-like property. Similar to thixotropy, the magnetic field-induced behavior is also reversible [16]. On one hand, the magnetic forces on nano-Fe_3O_4 particles decreased with the decrease of magnetic field strength, resulting in the disintegration of parts of column-like structure. On the other hand, the Brownian motion and electrostatic forces between solid particles gradually increased, and thus the reduction in storage modulus was observed. Comparing with the cementitious paste under constant magnetic fields, the slope of storage modulus with time was slightly higher for the cementitious paste after experiencing the decrease of magnetic field from high to lower value. For example, the storage modulus when the magnetic field decreased from 0.25 T to 0 T (i.e. $t = 600$ s) was almost similar to that obtained under constant magnetic field of 0 T. However, the difference in storage modulus between these two modes (black and green lines) was about 150 kPa at 900 s. This phenomenon can be explained by the magnetic properties of nano-Fe_3O_4 particles. After the magnetic field is removed, there exist residual chain-like structures formed at high magnetic fields, as shown in Fig. 6(c). As a result, the interactions between particles are enhanced. Thus, a higher growth rate of storage modulus was obtained for the cementitious paste after experiencing the changing magnetic field from high to zero.

3.3. Linearly-changed magnetic fields

From the above results, it can be concluded that both the sudden-increased and sudden-decreased magnetic fields resulted in a sharp

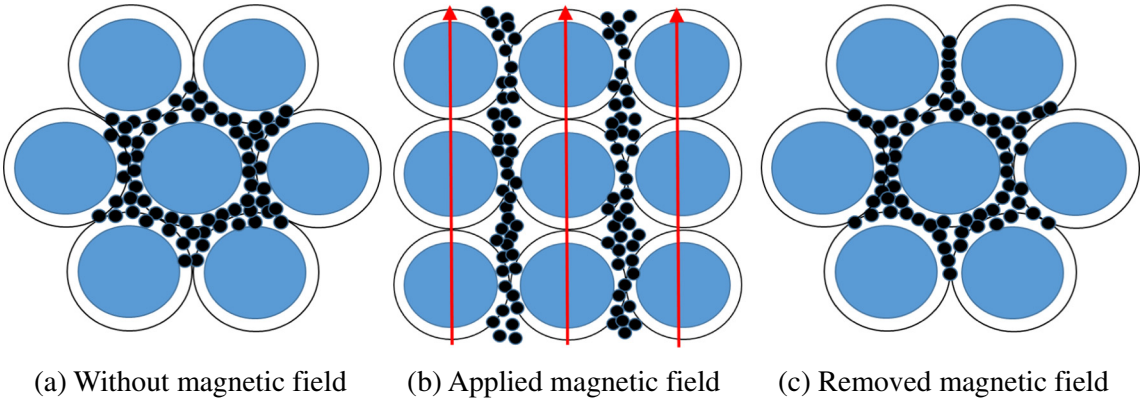

Fig. 6. Schematic diagram illustrating the distribution of nano-Fe_3O_4 in the cement paste matrix.

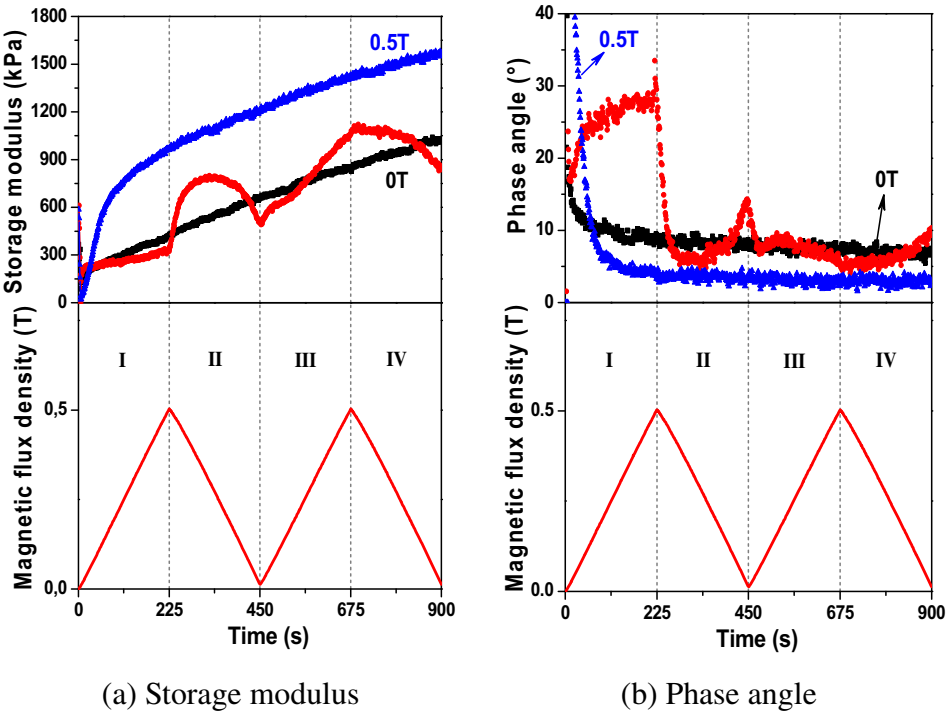

Fig. 8. Application modes of linearly-changed magnetic fields and their effects on the structural evolution of cementitious paste.

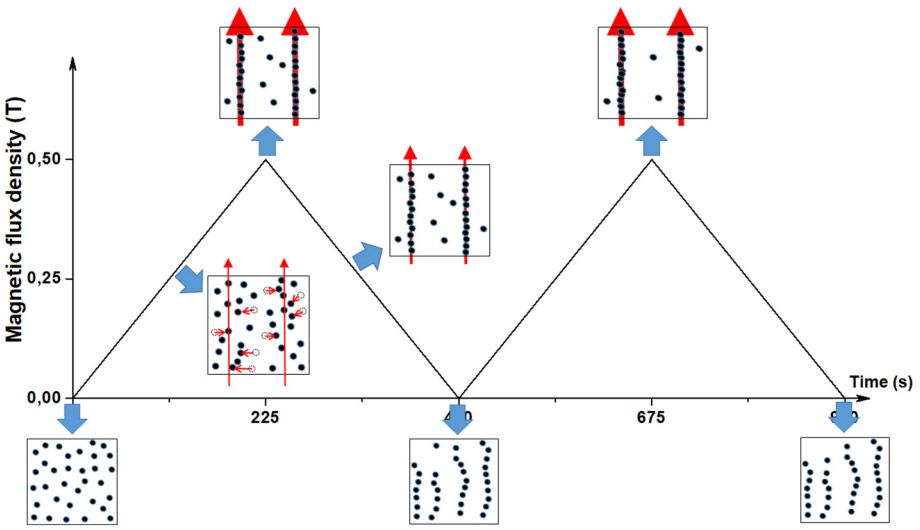

Fig. 9. Schematic diagram of nanoparticles distribution in cement paste matrix with the linearly-changed magnetic fields.

decrease in storage modulus. In this section, the influences of linearly-changed magnetic fields on the structural evolution of cementitious paste were evaluated, as shown in Fig. 8. With the linearly increasing magnetic field from 0 T to 0.5 T, the storage modulus increased slowly but a significant increase in phase angle was observed. This means that the linearly increasing magnetic field led to more viscous behavior. As mentioned before, the chain-like structure can be formed within a very short time under external magnetic fields. Indeed, the internal structure (flocculated and field-induced) formation and the magnetic nanoparticles movement are both existed simultaneously under external magnetic fields, as presented in Fig. 9. When the magnetic field linearly increased, on one hand, the movement of magnetic nanoparticles destroyed the connections between particles and promoted the cement particles to arrange orderly, which significantly improved the viscous behavior of cementitious paste. On the other hand, the magnetic nanoparticles gradually assembled along the direction of the magnetic field, which increased the capacity of stored energy (i.e. elastic behavior). During the linearly increasing magnetic field from 0 T to 0.5 T, the hydrodynamic and magnetodynamic forces dominated the attractive forces. In other words, the structural breakdown dominated the structural build-up, and therefore, an increase in phase angle was observed. At the time when the magnetic flux density was 0.5 T, the amount of magnetic nanoparticles used to form chain-like structure reached a maximum, and some part of nanoparticles might still contribute to the interstitial particle volume and not have reached the chain-like structure.

With the linearly decreasing magnetic field, it is expected that the storage modulus will decrease. However, Fig. 8(a) shows an increase in the storage modulus when the magnetic field linearly decreased from 0.5 T to approx. 0.25 T. This means that the structural build-up was enhanced and the nanoparticles did not exhibit agitation or movement. Indeed, the magnetic nanoparticles keep their chain-like structure

during the beginning of linearly decreasing magnetic fields, because the intrinsic viscoelastic behavior of the cement paste medium [38] and the magnetic fields is not low enough to break down the structure. Thus, the chain-like structure gradually consolidated due to the interactions between particles under the high magnetic field strength (from approx. 0.25 T to 0.5 T), as illustrated in Fig. 9. Furthermore, the magnetic nanoparticles that are free between cement particles do not need to move to form weaker chain-like structure when the magnetic field linearly decreased. In contrast, they keep their positions unchanged and enhance the inter-particle interactions. As a result, the storage modulus increased and the phase angle decreased dramatically with the linearly decreasing magnetic field from 0.5 T to approx. 0.25 T.

With the magnetic field linearly decreasing from approx. 0.25 T to 0 T, the magnetic field strength is not high enough to maintain the chain-like structure. The magnetic nanoparticles will try to redistribute and become chaotic again in the cement paste matrix. In this situation, the nanoparticles will move and agitate the cement paste matrix which leads to decrease in storage modulus. Thus, it can be concluded that the chain-like structure facilitates the interactions between the particles by increasing their contacts. But once the chain-like structure is destroyed, the movement of nanoparticles will break down the links between the particles and lead to a decrease in storage modulus. Compared to the initial value, a higher storage modulus was observed at 450 s, and the changes of storage modulus and phase angle at the second cycle were different from that at the first cycle when linearly changing the magnetic field. This indicates that the dynamic responses of cementitious paste exhibited a history dependency, which can be attributed to the differences in the structure of cement paste matrix. At the initial test, the cementitious paste was in a most de-flocculated state because of the pre-shearing process. While after the first cycle, the C-S-H networks, flocculated structure and residual field-induced chains existed in the cementitious paste. For these reasons, the magnetic nanoparticles suffer a higher movement resistance when linearly increasing the magnetic field again (i.e. Stage III). On the contrary, the magnetic nanoparticles in the surrounding residual chains could easily form column-like structure. As a result, the interactions between particles dominate the agitation effect of nanoparticle movements, and thus an increase in storage modulus was obtained at Stage III.

In order to clarify the proposed explanations, the continuous linearly-increased magnetic fields were applied to the cementitious paste and the evolution of storage modulus was recorded. As shown in Fig. 10, the external magnetic field increased from 0 T to 0.5 T within 300 s (step I). Afterwards, step I was repeated for two times. Compared with the cementitious paste under constant 0 T, lower storage modulus was expectedly obtained for the cementitious paste under the action of linearly increasing magnetic field. It should be noted that the reduction of storage modulus under linearly increasing magnetic fields was independent of the time duration. At 300 s, the magnetic field decreased from 0.5 T to 0 T, thus, an instant drop of storage modulus was observed. According to the hypotheses proposed in Fig. 9, the residual chains between magnetic nanoparticles would result in higher growth rate of storage modulus at step II, comparing with step I. Furthermore, when the magnetic field dropped from 0.5 T to 0 T, the storage modulus at 300 s should be slightly lower than that at 600 s due to the flocculated structure, early cement hydration and residual chains, and the growth rates of storage modulus at steps II and III should be similar because of the same mechanism of action. It can be observed from Fig. 10 that all the experimental results are consistent with the expected results.

4. Conclusions

In the present study, the structural evolution of cementitious pastes under time-varying magnetic fields was experimentally investigated. Based on the results and discussion, the following conclusions can be reached:

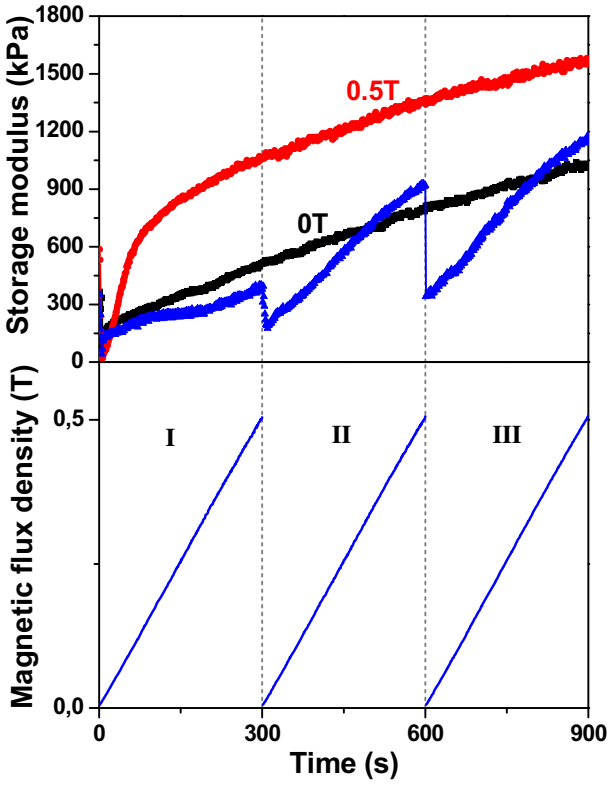

Fig. 10. Structural evolution of cementitious paste under continuous linearly-increased magnetic fields.

(1) The action of applying constant magnetic fields increased the percolation time and storage modulus at equilibrium state, and their changes were proportional to the magnetic field strengths. However, as the storage modulus is related to the colloidal interactions after the chain-like structure formed, the growth rate of storage modulus at equilibrium state is similar for different strengths of static magnetic fields.

(2) When the magnetic fields changed from zero to a higher value, the C-S-H bridges and flocculated networks between cement particles were destroyed by the movement of nanoparticles, and the entrained water in the agglomerated nanoparticle clusters was released. With the magnetic fields changing from low (not zero) to higher value, the nanoparticles in the existing chains will redistribute and the nanoparticles remaining in the gap between cement particles start to move to form chains or clusters, resulting in the breakdown of the C-S-H links.

(3) The decrease of magnetic field strength resulted in the disintegration of chain- or column-like structures, and a reduction in storage modulus was observed. After removing the magnetic fields, there exist residual chain-like structures in the cementitious paste, and thus a higher growth rate of structural build-up of cementitious paste.

(4) The structural build-up of cementitious paste under the linear magnetic field sweep mode was history-dependent. With the linearly increasing magnetic field, the agitation effect of nanoparticles movement dominated the formation of field-induced structure, leading to higher liquid-like behavior. When the magnetic field linearly decreased from 0.5 T to approx. 0.25 T, the nanoparticles stopped to move and the chain-like structures are kept intact because of the viscoelastic behavior of paste suspension. In this case, the inter-particle interactions consolidated the chain-like structures. With the continuously decreasing magnetic field from approx. 0.25 T to 0 T, the chain-like structures gradually disintegrated and increased the liquid-like properties.

Acknowledgements

The authors acknowledge the support given by the European Research Council (ERC) for the Advanced Grant Project 'SmartCast' (No. 693755) awarded to Prof. Geert De Schutter, as well as the financial support from National Key Research and Development Program of China (2017YFB0310100).

References

[1] C. Shi, Z. Wu, K. Lv, et al., A review on mixture design methods for self-compacting concrete, Constr. Build. Mater. 84 (2015) 387–398.
[2] D. Jiao, C. Shi, Q. Yuan, et al., Mixture design of concrete using simplex centroid design method, Cem. Concr. Compos. 89 (2018) 76–88.
[3] D. Kaplan, Pumping of Concretes, Ph-D dissertation (in French) Laboratoire Central des Ponts et Chausées, Paris, 2001.
[4] D. Feys, G. De Schutter, R. Verhoeven, et al., Similarities and differences of pumping conventional and self-compacting concrete, Design, Production and Placement of Self-Consolidating Concrete, Springer, 2010, pp. 153–162.
[5] S.H. Kwon, C.K. Park, J.H. Jeong, et al., Prediction of concrete pumping: part II—analytical prediction and experimental verification, ACI Mater. J. 110 (2013) 657–667.
[6] G. De Schutter, D. Feys, Pumping of fresh concrete: insights and challenges, RILEM Technical Letters 1 (2016).
[7] E. Secrieru, D. Cotardo, V. Mechtcherine, et al., Changes in concrete properties during pumping and formation of lubricating material under pressure, Cem. Concr. Res. 108 (2018) 129–139.
[8] G. De Schutter, Thixotropic effects during large-scale concrete pump tests on site, 71st RILEM Annual Week & ICACMS 2017 Chennai, India, 2017.
[9] N. Roussel, F. Cussigh, Distinct-layer casting of SCC: the mechanical consequences of thixotropy, Cem. Concr. Res. 38 (2008) 624–632.
[10] G. Ovarlez, N. Roussel, A physical model for the prediction of lateral stress exerted by self-compacting concrete on formwork, Mater. Struct. 39 (2006) 269–279.
[11] N. Roussel, A thixotropy model for fresh fluid concretes: theory, validation and applications, Cem. Concr. Res. 36 (2006) 1797–1806.
[12] G. De Schutter, K. Lesage, Active control of properties of concrete: a (p)review, Mater. Struct. 51 (2018).
[13] G. De Schutter, K. Lesage, V. Mechtcherine, et al., Vision of 3D printing with concrete—technical, economic and environmental potentials, Cem. Concr. Res. 112 (2018) 25–36.
[14] J. Rabinow, The magnetic fluid clutch, Electr. Eng. 67 (1948) 1167.
[15] I. Bica, Y.D. Liu, H.J. Choi, Physical characteristics of magnetorheological suspensions and their applications, J. Ind. Eng. Chem. 19 (2013) 394–406.
[16] M. Ashtiani, S.H. Hashemabadi, A. Ghaffari, A review on the magnetorheological fluid preparation and stabilization, J. Magn. Magn. Mater. 374 (2015) 716–730.
[17] G.H. Tattersall, P.F. Banfill, The Rheology of Fresh Concrete, (1983).
[18] M.A. Schultz, L.J. Struble, Use of oscillatory shear to study flow behavior of fresh cement paste, Cem. Concr. Res. 23 (1993) 273–282.
[19] D. Jiao, C. Shi, Q. Yuan, et al., Effect of constituents on rheological properties of fresh concrete—a review, Cem. Concr. Compos. 83 (2017) 146–159.
[20] M.A. Ahmed, M.Y. Hassaan, S. Mahrous, et al., Application of magnetic-susceptibility to study low iron substitution in tricalcium aluminate, J. Am. Ceram. Soc. 78 (1995) 1958–1960.
[21] R. Gopalakrishnan, S. Barathan, D. Govindarajan, Magnetic susceptibility measurements on fly ash admixtured cement hydrated with groundwater and seawater, American Journal of Materials Science 2 (2012) 32–36.
[22] S.D. Nair, R.D. Ferron, Set-on-demand concrete, Cem. Concr. Res. 57 (2014) 13–27.
[23] S.D. Nair, R.D. Ferron, Real time control of fresh cement paste stiffening: smart cement-based materials via a magnetorheological approach, Rheol. Acta 55 (2016) 571–579.
[24] H. Li, H.-g. Xiao, J. Yuan, et al., Microstructure of cement mortar with nano-particles, Compos. Part B 35 (2004) 185–189.
[25] A.H. Shekari, M.S. Razzaghi, Influence of nano particles on durability and mechanical properties of high performance concrete, Procedia Engineering 14 (2011) 3036–3041.
[26] M.S. Amin, S.M.A. El-Gamal, F.S. Hashem, Effect of addition of nano-magnetite on the hydration characteristics of hardened Portland cement and high slag cement pastes, J. Therm. Anal. Calorim. 112 (2012) 1253–1259.
[27] A.M. Rashad, A synopsis about the effect of nano-Al2O3, nano-Fe2O3, nano-Fe3O4 and nano-clay on some properties of cementitious materials – a short guide for Civil Engineer, Materials & Design (1980–2015) 52 (2013) 143–157.
[28] EN TS 196-1, Methods of Testing Cement–Part 1: Determination of Strength, European Committee for standardization, 2005, p. 26.
[29] A.M. Mostafa, A. Yahia, New approach to assess build-up of cement-based suspensions, Cem. Concr. Res. 85 (2016) 174–182.
[30] Q. Yuan, X. Lu, K.H. Khayat, et al., Small amplitude oscillatory shear technique to evaluate structural build-up of cement paste, Mater. Struct. 50 (2017) 112.
[31] L. Nachbaur, J. Mutin, A. Nonat, et al., Dynamic mode rheology of cement and tricalcium silicate pastes from mixing to setting, Cem. Concr. Res. 31 (2001) 183–192.
[32] N. Roussel, G. Ovarlez, S. Garrault, et al., The origins of thixotropy of fresh cement pastes, Cem. Concr. Res. 42 (2012) 148–157.
[33] Q. Yuan, D. Zhou, K.H. Khayat, et al., On the measurement of evolution of structural build-up of cement paste with time by static yield stress test vs. small amplitude oscillatory shear test, Cem. Concr. Res. 99 (2017) 183–189.
[34] N. Roussel, A. Gram, Simulation of Fresh Concrete Flow, RILEM State-of-the-Art Reports, (2014), p. 15.
[35] P. Sikora, E. Horszczaruk, K. Cendrowski, et al., The influence of nano-Fe3O4 on the microstructure and mechanical properties of cementitious composites, Nanoscale Res. Lett. 11 (2016) 182.
[36] N. Su, Y.H. Wu, C.Y. Mar, Effect of magnetic water on the engineering properties of concrete containing granulated blast-furnace slag, Cem. Concr. Res. 30 (2000) 599–605.
[37] N. Su, C.-F. Wu, Effect of magnetic field treated water on mortar and concrete containing fly ash, Cem. Concr. Compos. 25 (2003) 681–688.
[38] P.J. Rankin, A.T. Horvath, D.J. Klingenberg, Magnetorheology in viscoplastic media, Rheol. Acta 38 (1999) 471–477.